energies

MDPI

Article

Optimal Dynamic Reactive Power Reserve for Wind Farms Addressing Short-Term Voltage Issues Caused by Wind Turbines Tripping

Liang Wu [1,*], Lin Guan [1,*], Feng Li [1,2], Qi Zhao [3], Yingjun Zhuo [1], Peng Chen [4] and Yaotang Lv [5]

1 School of Electric Power, South China University of Technology, Guangzhou 510640, China; lifeng@gd.csg.cn (F.L.); swzyj624@163.com (Y.Z.)
2 Guangdong Power Grid Co., Ltd., Guangzhou 510080, China
3 Logistics Center of Guangdong Power Grid Co., Ltd., Guangzhou 510630, China; zhaoqi_916@163.com
4 Electric Power Research Institute of Guangdong Power Grid Co., Ltd., Guangzhou 510080, China; chenpp2018@163.com
5 Power Dispatching and Control Center of China Southern Grid, Guangzhou 510000, China; traccce_tam@163.com
* Correspondence: scutwuliang@foxmail.com (L.W.); lguan@scut.edu.cn (L.G.); Tel.: +86-20-8711-3233

Received: 10 May 2018; Accepted: 20 June 2018; Published: 1 July 2018

Abstract: In regional power grids with high wind power penetration, wind turbine tripping poses great challenges to short-term voltage stability. Dynamic reactive power (VAR) compensation (DVC) plays an important role in securing wind farm operation. To address short-term voltage stability issues, voltage disturbance index (DI) and voltage supporting index (SI) are defined to evaluate the degree of voltage fluctuation and voltage supporting ability of a bus, respectively. Then corresponding vector-type features, called disturbance vector (DV) and supporting vector (SV) are proposed based on the defined indexes. The Kendall rank correlation coefficient is adopted to evaluate the matching degree of DV and SV, so as to determine the influenced area of each wind farm. Candidate locations for DVC are determined sequentially. By comprehensively considering the probability of combined disturbance in each wind farm, a site selection method is proposed and then genetic algorithm is applied to optimize the DVC capacity considering short-term voltage security. The proposed method is applied on a modified NE 39-bus system and a real power grid. Comparison with the engineering practice-based method validates its effectiveness.

Keywords: dynamic VAR compensation; short-term voltage stability; wind turbines tripping; Kendall rank correlation coefficient

1. Introduction

Wind power is attracting increasing attention across the world. In China, major load areas are far from large-scale wind farms; as a result, wind power is often collected to the point of common coupling (PCC) and then centrally transmitted to load areas [1]. However, in recent years, as small-scale offshore and near-sea wind farms have developed rapidly in coastal areas, wind power is now dispersedly integrated into regional power grids [2]. In this situation, the synchronous stability issue has diminished, while short-term voltage stability issues brought by power fluctuation are becoming significant due to the stochastic nature of wind speed, especially in radial grids without local synchronous power supplies [3]. In coastal areas where typhoons hit frequently, wind turbine tripping due to excessive wind speed often occurs; with the increase of installed capacity of wind power, the resulting impacts can no longer be neglected [4].

Voltage stability issues caused by wind power fluctuation can be grouped into two categories: static voltage stability and transient voltage stability issues. Existing research mainly focuses on static voltage stability problems resulting from wind power fluctuation in terms of hour and minute time scales, e.g., [5,6]; while transient voltage stability issues are generally studied under short-circuit fault scenarios [7], i.e., transient voltage stability issues caused by disturbances arising from the wind turbines themselves are rarely considered. Once the wind speed is over the cut-off speed, some wind turbines would trip off. In this situation, as the slow-response capacitor banks cannot switch off in time, the wind farm's voltage could rise to a certain high level and may result in cascading tripping [8,9].

Although the hierarchical automatic voltage control (AVC) system can support rational voltage profiles considering the intermittent and stochastic characteristics of wind power [10], it still requires sufficient dynamic reactive power (VAR) reserve to provide rapid dynamic VAR support when wind turbine tripping occurs [11]. With this concern, power system usually requires sufficient dynamic VAR compensation capacity to be mandatorily installed in the wind farms. Hence, most of the recently built wind farms in China coastal areas are equipped with dynamic VAR compensators (DVC), e.g., Static Synchronous Compensator (STATCOM), Static Var Compensator (SVC), etc. which significantly increase the total investment cost of the wind farms. Effective planning of the locations and capacity of the DVCs from the system perspective can greatly reduce the investment on DVCs and promote wind farm integration ability.

DVC planning aims at dealing with short-term voltage stability issues using DVC devices with the least investment [12]. Currently, DVC planning mainly focuses on short-circuit fault scenarios, which can be divided into two inter-related steps: site selection and capacity optimization. Site selection plays a major role in DVC planning, which determines the optimality of the overall planning scheme. Trajectory sensitivity index (TSI) is widely applied to identify proper installation locations with sufficient control ability [12–14]. After calculating the TSI regarding voltage dip, low voltage duration, etc. to reactive power injection, buses with strong control ability are distinguished via a ranking method. However, due to the proximity effect of the voltage dip, adjacent buses tend to be simultaneously selected by the TSI ranking based methods, resulting in redundant installation. To overcome this shortcoming, a zoning-based approach is put forward in [15,16], which partitions the grid and then determines installation locations by zones.

Capacity optimization is another crucial step following sites selection. As it is computationally expensive, existing references provided two typical optimization strategies: two-stage optimization [13,17] and full optimization [18]. The two-stage optimization approach determines the locations and capacity separately, which is widely adopted due to its less computational complexity. However, its optimality is consequently sacrificed. The full optimization approach optimizes locations and capacity simultaneously for better optimality, generally using intelligent searching algorithms, e.g., Particle Swarm Optimization (PSO), Genetic Algorithm (GA), etc. while due to its huge computation load, it may be hard to solve or even infeasible in a large-scale system. Thus, in engineering practice, the former one is a priority selection and at this point, determining proper locations is of great concern.

As short-term voltage stability issue induced by wind turbine tripping is becoming critical, and few articles deals with it, this paper develops a DVC planning strategy considering wind turbine tripping, so as to restrain transient voltage fluctuations to prevent cascading tripping. Note that as wind turbine tripping is a kind of non-Gaussian intermittency [19,20], it is rational to consider the worst condition in the planning stage. The so-called worst conditions would vary depending on the interest of different studies. In our framework, we focus on the dynamic reactive power reserve for wind farms. Therefore, in our proposed framework, we consider the worst condition which will cause severe short-term voltage stability issues. This situation usually refers to the early morning scenario, where the load is light but the wind turbines almost work at rated condition. In this case, the requirement of dynamic reactive power would be great due to the few synchronous generators providing dynamic reactive power support. In this scenario, once wind turbines are tripped, the power imbalance will greatly influence the power flow and lead to short-term voltage stability issues. Dynamic reactive power reserve considering this scenario is sufficient for other scenarios. The contributions of this paper are summarized as follows:

(1) A vector-type evaluation indexes system is established, including Disturbance Vector (DV) to assess the influence of wind power large disturbance on system-wide transient voltage; and Supporting Vector (SV) to evaluate a bus's system-wide transient voltage control ability.
(2) The Kendall rank correlation coefficient of DV and SV is calculated and then the grid is partitioned into several parts to differentiate the influenced areas of each wind farm, which helps reduce searching the space for candidate locations.
(3) A novel DVC planning scheme is put forward for preventing cascading tripping of wind farms. Based on the above indexes, combined disturbances and their probability are considered to determine proper installation locations. Then, a genetic algorithm is introduced to optimize DVC capacity, considering the transient voltage constraints to prevent cascading tripping.

The rest of the paper is organized as follows: Section 2 establishes the indexes system including DV and SV to evaluate buses' transient voltage behavior. Based on the indexes system, a novel DVC planning scheme is proposed in Section 3, and the sites selection and the capacity optimization steps are provided in detail. Section 4 provides a case study on a modified NE 39-bus system and application on a real regional grid in Southern China is conducted in Section 5. Conclusions are given in Section 6.

2. Evaluation on Buses' Transient Voltage Behavior

In this section, vector-type indexes describing buses' transient voltage fluctuation and voltage control ability are defined, respectively. The vector-type indexes record buses' dynamic characteristics more completely thus provide more information in analysis. Note that the proposed indexes are universal, which can be also applied in other scenarios, e.g., short-circuit faults.

2.1. Voltage Disturbance Index

Once an extremely strong wind, e.g., a typhoon, occurs, the wind turbines would be tripped off by its protection system, resulting in a large amount of unbalanced power. Synchronous generators will then adjust their output to balance the system-wide power flow. Consequently, the change of power flow lead to voltage fluctuation on each bus with varying degree. The difference of voltage fluctuation is reflected in fluctuation amplitude and time duration. To comprehensively consider the above factors, the Disturbance Index (*DI*) is defined as in (1):

$$DI = \int_{t_0}^{t_e} |V_t - V_0| dt \tag{1}$$

As shown in Figure 1, *DI* is denoted by the shaded area, reflecting the accumulation of voltage amplitude deviation from steady state value within a certain time span.

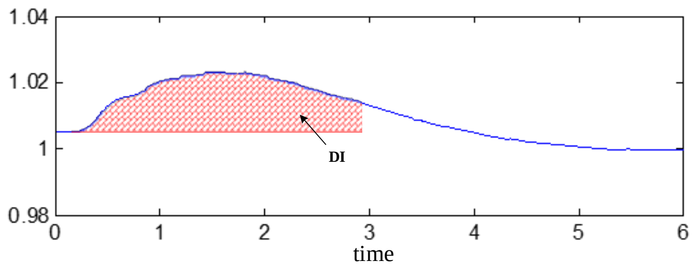

Figure 1. Illustration of *DI*.

To globally characterize the system-wide influence of a disturbance, Disturbance Vector (***DV***) is defined as in (2):

$$\boldsymbol{DV} = [DI_1, DI_2, \ldots, DI_N] \tag{2}$$

where 1, 2, ... , N is the bus number.

The ***DV*** index retains the *DI* value of each bus under the corresponding disturbance scenario. Therefore, compared with the widely-used scalar-type index, ***DV*** can record more information and thus serves as the influencing feature of the disturbance scenario in our study.

2.2. Voltage Supporting Index

A bus's voltage will deviate from its specified value when a contingency occurs. Then, a DVC source will quickly respond to absorb or inject reactive power to reduce the degree of voltage fluctuation. DVC planning aims at providing a rational DVC allocation scheme to secure the power system operation on the premise of the economy.

To quantify the compensation effect of a DVC device, we define Supporting Index (*SI*) in Equation (3) and its specific meaning is provided in Figure 2:

$$SI_{ij} = \left| \int (V'_j - V_j) dt \right| \tag{3}$$

where the reactive power signal duration is set as 2~6 s; the amplitude of reactive power signal is determined by testing, with which the maximum voltage improvement is about 0.2 pu to 0.4 pu.

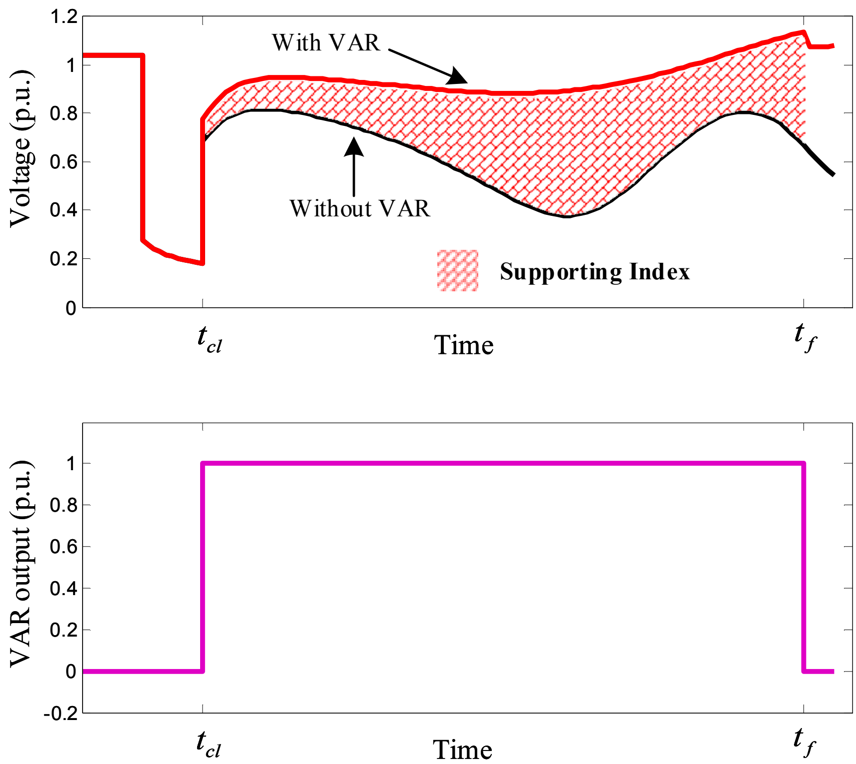

Figure 2. Definition of *SI* index.

As shown in Figure 2, the SI represents the accumulation of voltage improvement in time domain thus can be used to evaluate buses' voltage control ability.

Analogous to the definition of DV, here we use SI to constitute a new vector-type index Supporting Vector ($\boldsymbol{SV}$) as given in (4):

$$\boldsymbol{SV}_i = [SI_{i1}, SI_{i2}, \ldots, SI_{iN}] \tag{4}$$

where SI_{ij} represents the voltage improvement of bus j with reactive power injection on bus i. Therefore, the SV index records the system-wide control ability of a specific bus.

Note that SI value is related to three factors: contingency, the controlling bus (i.e., the bus with reactive power injection) and the controlled bus. Hence, the $\boldsymbol{SV}$ value of a certain bus varies with contingencies. So far, we have built a vector-type indexes system to characterize the influence of disturbance and voltage control ability of buses, respectively. The DVC planning method based on the above indexes system will be described in the following sections.

3. DVC Planning Model

In the existing literatures, DVC planning is mainly applied to solve the problem of large disturbances such as short-circuit faults. The basic framework is as follows: firstly, determine the security range of transient voltage according to operation guidelines. Then select proper locations for DVC allocation and optimize capacity to ensure that transient voltage of all the buses subject to considered faults are all within their security range, at the same time with the least investment. Our study follows the similar framework and takes the wind turbines tripping as the disturbance scenario to carry out DVC planning. It is to be noted that our proposed method is based on simulation results, i.e., we can use any specific simulation models as we need to make a trade-off between the accuracy of the results and the computational cost.

3.1. Objective and Constraints

DVC planning is a mix-integer nonlinear programming problem. Its objective is to minimum the total investment as given in (5):

$$\min f = \sum_{i=1}^{N} \omega_i \left(Q_i C_{\text{var}} + C_{fix} \right) \tag{5}$$

where $\omega \in \{0, 1\}$ denotes whether the corresponding bus is selected for compensation; Q_i is the DVC capacity on bus i; C_{var} is the unit variable cost and C_{fix} is the fixed cost of DVC installation. In this study, C_{fix} = \$1.5 million, C_{var} = \$5 million/100 MVar.

Considering the operation security, the constraints are provided in (6) to (8):

$$\begin{cases} x = f(x, y, u, s) \\ 0 = g(x, y, u, s) \end{cases} \tag{6}$$

$$V_{low}(t) < V(t) < V_{up}(t) \forall t \in [t_{cl}, t_{end}], i = 1, 2 \ldots, N, j = 1, 2, \ldots, K \tag{7}$$

$$0 \leq Q_i \leq Q_{\max} \tag{8}$$

where $x \in \boldsymbol{R}^{N_x}$ represents the state variables; $y \in \boldsymbol{R}^{N_y}$ represents the algebraic variables; $u \in \boldsymbol{R}^{N_u}$ represents the control variables; $s \in \boldsymbol{R}^{N_s}$ represents parameters of reactive power compensation devices; f, g are the dynamic state function and power flow function, respectively; (8) is the capacity constraint considering the expensive cost of large capacity DVC devices; V_{low} and V_{up} are voltage boundaries, whose value is determined according to system operation requirements and in our study focusing on transient voltage security after wind turbines tripping, the boundaries are as recommended in (9) considering the operation requirements of wind turbines. Note that as different type of wind turbines have different operation requirements, the boundaries can be adjusted in real applications:

$$0.9\text{p.u.} \leq V(t) \leq 1.1\text{p.u.} \tag{9}$$

In addition, we define Voltage Violation Index (VVI), as given in (10) to denote the integral of over-limit voltage in time domain:

$$\begin{aligned} VVI &= \int_{t_{cl}}^{t_{end}} v'(t)dt \\ v'(t) &= \begin{cases} (V_{low} - V(t))/V_0, \text{ if } V(t) < V_{low} \\ (V(t) - V_{up})/V_0, \text{ if } V(t) > V_{up} \\ 0, \quad \text{otherwise} \end{cases} \end{aligned} \tag{10}$$

Hence, (7) can be rewritten as given in (11):

$$\sum_{i=1}^{N}\sum_{j=1}^{K} VVI_{ij} = 0 \tag{11}$$

Then we can obtain the equivalent representation of the optimization problem in (12):

$$\min g = \sum_{i=1}^{N} w_i \left(Q_i C_{\text{var}} + C_{fix} \right) + M \left(\sum_{i=1}^{N}\sum_{j=1}^{K} VVI_{ij} \right)^2 \tag{12}$$

where M is a large enough positive number to make the objective as large as possible when constraints are not satisfied. In this paper, $M = 1 \times 10^7$.

3.2. Selection of Installation Locations

In DVC planning, it is preferred to provide sufficient reactive power support to the seriously influenced buses. Note that to achieve this goal, SV and DV established in Section 2 provide a valuable guide for the site selection, which should be comprehensively considered. Then, in this section, the Kendall rank correlation coefficient is introduced to determine the best installation locations.

3.2.1. Kendall Rank Correlation Coefficient

There are various statistical indicators for measuring correlations between data sequences, e.g., the Pearson correlation coefficient and the linear correlation coefficient. However, they may be ineffective in the presence of noise, measurement inaccuracy, etc. Furthermore, we only focus on the relative positions of the elements in a sequence in this field, i.e., focus on their rank correlation. With this concern, Kendall rank correlation coefficient is widely used and proved to have great sensitiveness and discriminative ability [21,22].

Let X and Y be vectors, represented by $\{x_1, x_2, \ldots, x_n\}\{y_1, y_2, \ldots, y_n\}\ \forall i \neq j, x_i \neq x_j, y_i \neq y_j$.

Then, calculate conformance value (assumed by A) of each pair of elements by (13):

$$A_{ij} = \text{sgn}(x_i - x_j)\text{sgn}(y_i - y_j), i \neq j \tag{13}$$

That is, if the ranks of (x_i, x_j) and (y_i, y_j) are identical, $A_{ij} = 1$ means that they are concordant. Otherwise, if one ranking is the reverse of the other, $A_{ij} = -1$ means they are discordant.

The n-dimensional vectors can make up $n(n-1)/2$ pairs of elements and then calculate all the A value to compute Kendall correlation coefficient as given in (14):

$$\tau = \frac{\sum_{i=1}^{n}\sum_{j=1, j\neq i}^{n} A_{ij}}{n(n-1)/2} \in [-1, 1] \tag{14}$$

where $\tau = 1$ means that the ranking of the two sequence all identical; while $\tau = -1$ indicates that the ranking of one is the reverse of another; $\tau = 0$ denotes that they are completely independent.

3.2.2. Selection of Installation Locations

In a wind farm cluster, tripping disturbance of any combination of wind farms may cause different voltage violation issues. In addition, as mentioned before in Section 2, buses' voltage supporting ability (denoted by SV) varies with the disturbance. Therefore, it is crucial to select comprehensively optimal installation locations to cope with potential tripping disturbance.

In our study, probability of each potential disturbance scenario is considered to determine installation locations. Figure 3 provides a detailed illustration of the steps.

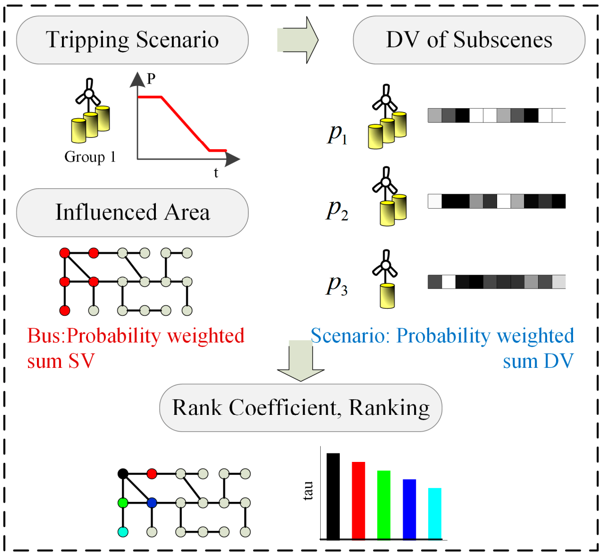

Figure 3. Sites selection for dynamic VAR considering probability of sub-scenario in each zone.

Firstly, according to geographical location and historical wind speed data, determine the potential tripping scenarios and their corresponding probability.

Subsequently, calculate DV vector of each considered scenario and then the probability-weighted sum is carried out to obtain a comprehensive vector $\boldsymbol{DV}_0$ in (15). Similar calculation is applied to get $\boldsymbol{SV}_0$ in (16):

$$\boldsymbol{DV}_0 = \frac{\sum p_i \boldsymbol{DV}_i}{\sum p_i} \tag{15}$$

$$\boldsymbol{SV}_{0,j} = \frac{\sum p_i \boldsymbol{SV}_{ij}}{\sum p_i} \tag{16}$$

where $\boldsymbol{DV}_i$ is the $\boldsymbol{DV}$ of scenario i; $\boldsymbol{SV}_{ij}$ is the $\boldsymbol{SV}$ of bus j in scenario i; p_{i} is the probability of scenario i.

Finally, we calculate the Kendall rank correlation coefficient of $\boldsymbol{DV}_0$ and $\boldsymbol{SV}_0$, then rank them in descending order. The bus with the greatest correlation coefficient is selected as the installation location for the corresponding wind farm cluster.

3.3. Capacity Optimization

The capacity optimization step purpose is to determine the DVC capacity considering operation security constraints with the least investment. Based on the selected locations, any feasible optimization algorithm, e.g., particle swarm optimization (PSO), genetic algorithm (GA), can be adopted. In this study, we use GA for capacity optimization.

The flow diagram for solving this is shown in Figure 4. The DAEs' constraints (6) are solved by a power system simulation tool (e.g., PSD-BPA) and the GA is run in MATLAB. The simulation tool provides a voltage series to MATLAB to transform into a penalty item in (12), then the original problem can be solved by the GA solver directly.

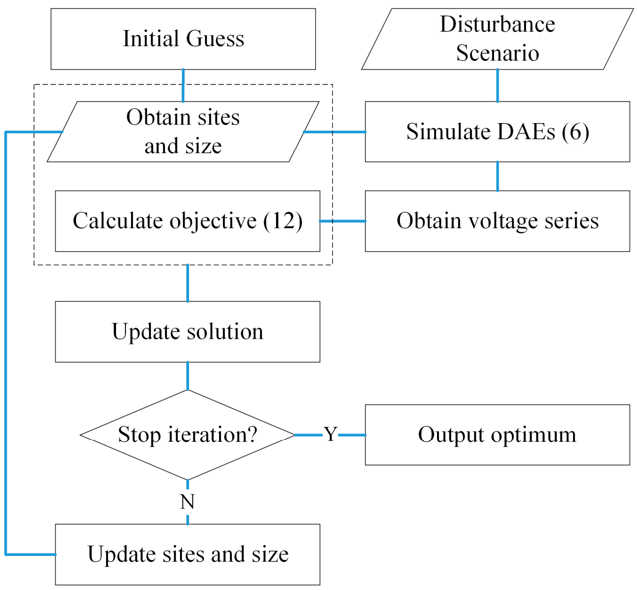

Figure 4. Flowchart of the proposed method.

4. Case Study on the Modified NE 39-Bus System

4.1. Simulation Settings

The original NE 39-bus system is modified considering high penetration wind power as shown in Figure 5. Thermal power plants in bus 33, bus 35 and bus 38 are replaced by a 600 MW wind farm (consisting of 400 1.5 MW wind turbines), respectively. In addition, generation in bus 36 is shut down and three small-capacity wind farms are added to bus 2, bus 8 and bus 9, respectively. The capacity of WF5 and WF6 is 49.5 MW; WF4 is 99 MW.

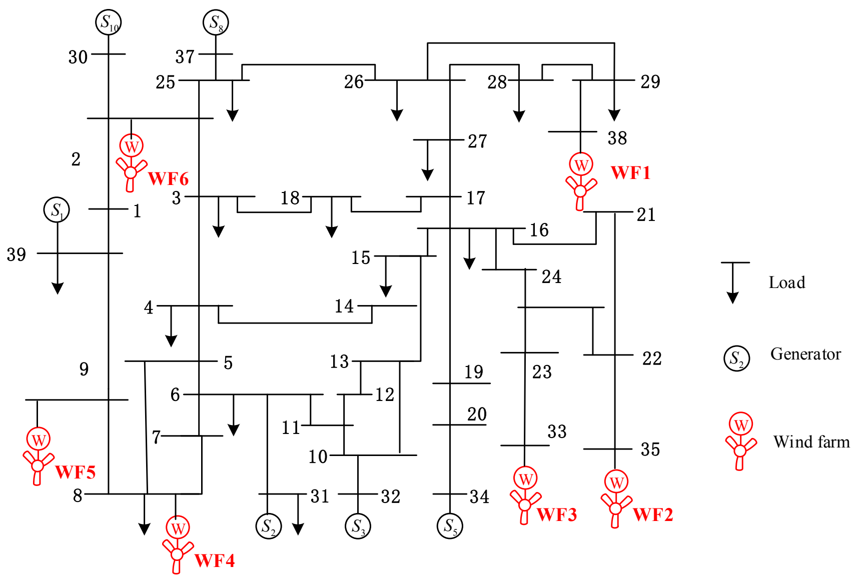

Figure 5. The modified NE 39-bus system with distributed large-scale wind farms.

An early morning scenario is considered, where the load is light and the wind turbines work at their rated condition; the load is 3800 MW and the wind power output is 1800 MW (the power factor is 0.95). The proportion of wind power is about 50%. Electricity production consists of 2000 MW thermal power and 1800 MW wind power.

A typhoon is simulated which causes 80% of the wind turbines in the wind farm trip off at 0.1 s. In this situation, the wind power output decreases to 20%. Other settings and parameters are provided in Table 1.

Table 1. Setting and parameters.

Model	Setting
Generator model	Fifth-order synchronous generator model
Load model	ZIP load and induction motor
Wind turbine	DFIG from GE company
Dynamic VAR source	Typical STATCOM in [23]

4.2. Locations Selection

For this system, the simulation results show that due to the small capacity of WF4, WF5 and WF6, wind turbines tripping disturbance occurred in these wind farms do not lead to significant voltage violation; therefore, only the three large-scale wind farms WF1~3 are considered in DVC planning.

According to geographical location and historical wind speed data, two tripping scenarios are taken into account, including wind turbines tripping in WF1, wind turbines tripping in WF2&3 (which means that the strong wind can cause tripping disturbance in both WF2 and WF3 simultaneously). Their SV and DV indexes are calculated and then their rank correlation coefficient is presented in Figure 6.

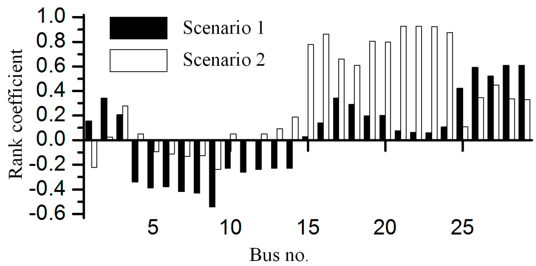

Figure 6. Rank correlation coefficient of DV and SV.

As shown in Figure 6, in scenario 1, the buses with large rank correlation coefficient include bus 25~29, among which bus 29 has the largest compensation ability to scenario 1. Therefore, bus 29 is selected as compensation location for addressing scenario 1.

For WF2&3, as we have referred above, there are three sub-scenarios in this wind farm combination:

Probability of disturbance only in WF2 or WF3 is 0.05;
Probability of disturbance in both WF2 and WF3 is 0.035.

Select bus 15~24 as candidate locations according to Figure 6, then calculate their comprehensive vectors and rank correlation coefficients. The result is shown in Figure 7 in greyscale image, where a dark color denotes a bigger value.

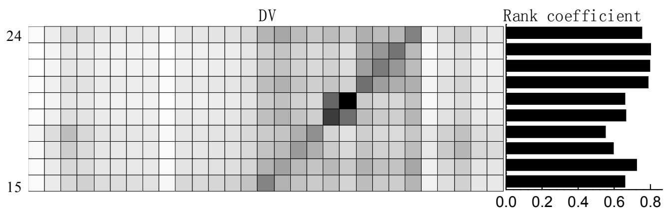

Figure 7. Rank correlation coefficient of DV and SV.

It can be found that bus 23 is comprehensively optimal; therefore, it is selected as compensation location for addressing scenario 2.

4.3. Capacity Optimization

Although the synchronous generators can provide the imbalanced active power caused by wind turbine tripping, it still requires dynamic VAR support because the great change of power flow causes a short-term voltage issue. In this case study, (9) is used as constraint and it requires that the time duration of voltage violation should not exceed 10 cycles (0.2 s). A widely used STATCOM [23] model is used as DVC device. GA is adopted to optimize the DVC capacity and considering the discreteness of capacity, 10 MVar is taken as the unit for capacity. Besides, we set the maximum capacity as 500 MVar due to the much higher cost of large-capacity DVC device.

The optimization result is to allocate 140 MVar and 120 MVar in bus 23 and bus 29, respectively. Simulation results show that the voltage violation issues caused by tripping disturbance have been well coped with after compensation. The voltage trajectories are compared in Figure 8, where the red dotted line is the upper limit.

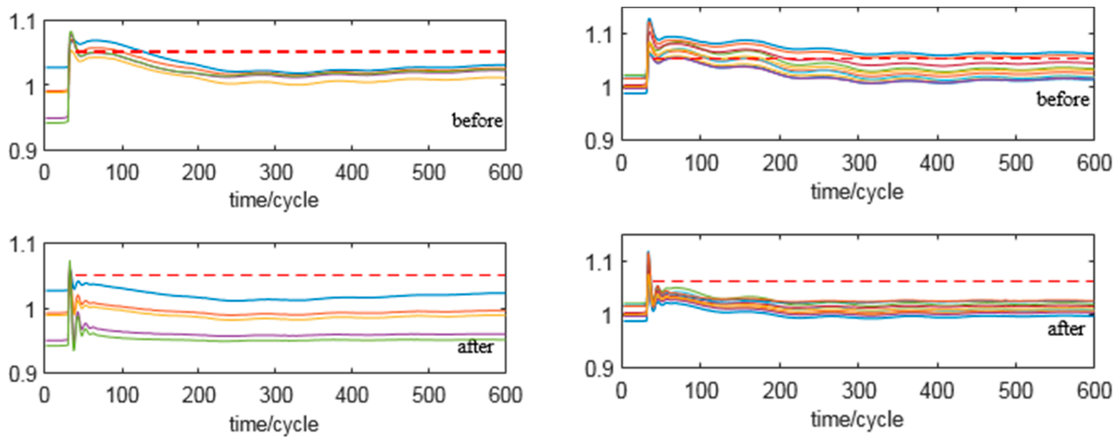

(a) **(b)**

Figure 8. Voltage trajectory before/after compensation. (**a**) Scenario 1; (**b**) Scenario 2.

As shown in Figure 8, before dynamic VAR compensation, the wind turbine tripping will cause short-term voltage violation. The provided optimal dynamic VAR compensation scheme can address well the short-term voltage issues; thus, the DVC source, i.e., STATCOM, can provide reactive power well to reduce violations to ensure short-term voltage stability.

5. Real Application in Southern China

A real application on a regional grid (ZJ grid) in Southern China is carried out. According to the planning data, there will be 25 wind farms integrated into the ZJ grid by 2020 and the total installed capacity will be 1730 MW. The peak load is forecasted to reach 5400 MW in the ZJ grid in 2020 and its grid structure is shown in Figure 9.

According to the analysis of the wind power correlation, the correlation coefficient of wind power output in the ZJ coastal area is significantly high and the peak output scenarios often appear in the early morning, typically at 5:00 a.m. in summer. The load level at 5:00 is 53% of the peak load, i.e., 2860 MW. Wind turbines work at 90% of the rated capacity and in this situation the proportion of wind power is 54.5%.

As ZJ is located in a typhoon-prone region, according to wind speed data, we consider 70% of the wind turbines collected into the same 220 kV bus trip off and the wind power decreases from 90% to 20%.

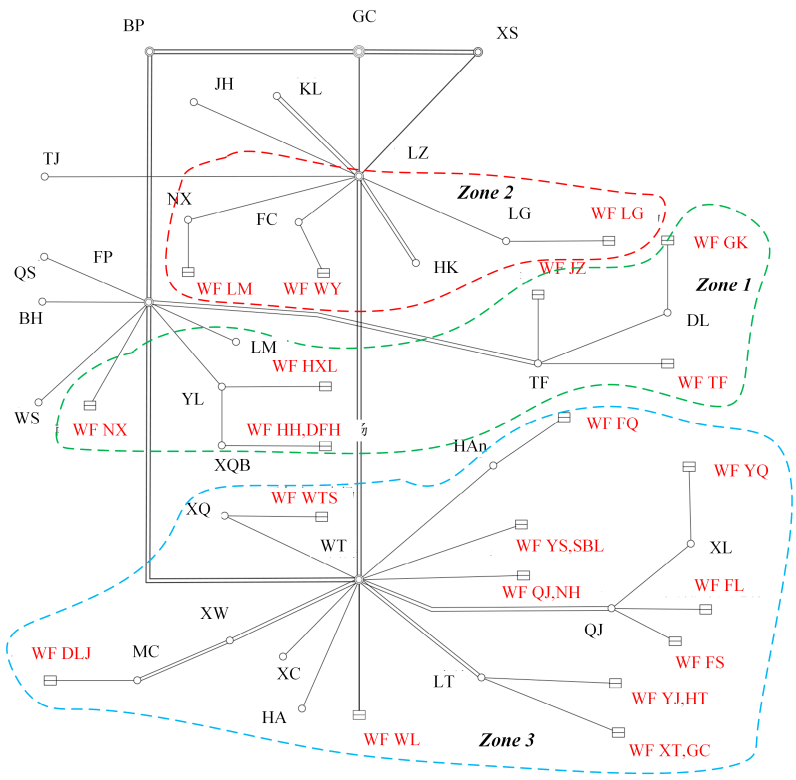

Figure 9. Structure of ZJ 110 kV and above power grid.

5.1. DVC Planning

The 25 wind farms are divided into three clusters according to the connected 220 kV substations. Only 110 kV buses are considered for DVC. A wind turbine tripping disturbance is simulated and the influenced areas of each clusters are provided in Table 2.

Table 2. Influence areas of each wind farm cluster.

Region	Influenced Buses No.
Zone 1	4 6 7 8 11 13 21 22 23 28 43 44 45 53 62 69 71 78
Zone 2	9 50 16 10 34 40 39 61
Zone 3	1–5 12 14 15 17–20 29 32–38 46–47 54 65 66 70 74–77

According to geographical location and historical wind speed data, the considered disturbances are as follows:

(1) Tripping disturbance happened in each wind farm, with probability 0.05;
(2) Only geographically close wind farms are considered for simultaneous disturbance and these combinations are given in Table 3.

Table 3. The considered disturbance scenario and its probability.

WF Combination	Probability
WF HH & DHF	0.03
WF QJ & NH	0.03
WF YS & SBL	0.03
WF YJ & HT	0.03
WF XT & GC	0.03

Based on the above scenarios, rank correlation coefficients of SV_0 and DV_0 in each cluster are calculated, and the results are shown in Figure 10.

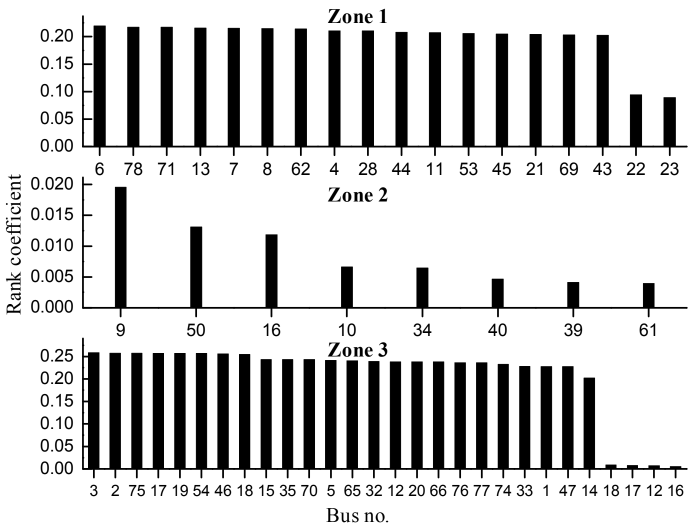

Figure 10. Rank correlation coefficient of DV and SV.

As Figure 10 shows, except for #22 and #23, other buses in zone 1 have a similar rank correlation coefficient value; therefore, further study on their voltage violation is performed.

In zone 2, #9 has the strongest compensation ability and in zone 3, the top 8 buses have similar rank correlation coefficient value. Therefore, further study is required. Using (9) as limits, the buses exceeding the limits are given in Table 4.

Table 4. The number of buses with voltage exceeding boundary.

Scenario	Buses No.
Zone 1	null
Zone 2	null
Zone 3	2 3 75 17 19 54 46 18 15 35
	70 5 65 32 12 20 66 76 77 74 33 1 47

We can find that only the disturbance in zone 3 will cause a voltage violation. The main reason is that zone 1 and zone 2 are closely connected to the GC 500 kV substation. Thus, the voltage of buses in these zones is well controlled, however, zone 3 is located at the end of the gird, with a weak connection to the main grid. In addition, the installed capacity of wind farms in this zone is significantly large. Therefore, the voltage violation is significant under disturbance conditions. With this concern, only zone 3 requires DVC.

The planning result is to allocate 20 MVar STATCOM on #2 (PCC of WF FL), the one with the strongest compensation ability. The reason is that there are several wind farms (FS, YQ, etc.) and when strong wind weather occurs, the tripping will cause a large capacity power fluctuation. Then, DVC on #2 can well cope with the voltage issue.

5.2. Comparisons and Discussion

This paper proposes a heuristic DVC planning method based on transient voltage behavior. Installation locations are determined by their voltage control ability. To validate the effectiveness of the proposed method, an engineering experience-based method is carried out.

According to engineering experience, #65 (named WT) is selected as installation location because it is the pivotal 220 kV substation of all the 110 kV lines in zone 3, indicating that it has the strongest control ability to its radial 110 kV substations. Then capacity optimization is accomplished and the result is to allocate 40 MVar STATCOM on #65 to address the voltage violation.

Comparison with the proposed method indicates that the capacity is relevant to the selected locations and it can be found that the proposed method is control ability oriented, which considers the matching degree and the bus voltage control ability and influence of disturbance; while the traditional method considers the central control capacity of the central station but neglecting the imbalance of capacity and location of wind farms. It can be seen from the results of capacity optimization that the proposed scheme can meet the same transient voltage constraints with less capacity, which shows that the proposed scheme is feasible and efficient.

6. Conclusions

This paper proposes a DVC planning method considering wind turbine tripping in regional power grids. A vector-type indexes system is established to evaluate buses' transient voltage features, including disturbance vector (DV) and supporting vector (SV). Then the Kendall rank correlation coefficient is adopted to evaluate the matching degree of SV and DV, so as to determine the best installation locations. Capacity optimization is subsequently accomplished. The proposed vector-type indexes retain more complete information, thus perform better than the widely-used scalar-type indexes. In addition, rank correlation coefficient of DV and SV is used to determine locations, which provides better locations because it considers the control effect of DVC. The adopted method is simulation based, thus can consider different parameters of wind turbine, generators and any other essential devices to provide a solution of greater accuracy. As the proposed framework is simulation-based, future work can focus on the mechanism of the influence of wind turbines tripping to provide more theoretical explanations to improve our approach. In addition, more scenarios considering the uncertainty characteristics of wind power can be applied for better performance. In short, the proposed framework provides an effective solution to optimal dynamic reactive power planning considering wind turbines tripping. Furthermore, the proposed method is transferable and can be applied to issues considering short-circuit fault and so on.

Author Contributions: L.W. and L.G. developed the framework and proposed the solving methods. F.L., Q.Z., Y.Z., and P.C, Y.L. helped in data analysis.

Funding: This research was funded by the National Natural Science Foundation of China grant number 51577071, China Southern Power Grid grant number CSGTRC-K163007 and Guangdong Natural Science Foundation grant number 2015A030313202.

Conflicts of Interest: The authors declare no conflict of interest.

Abbreviations

VAR	Reactive power
DVC	Dynamic VAR Compensation
PCC	Point of common coupling
AVC	Automatic voltage control
TSI	Trajectory sensitivity index
PSO	Particle swarm optimization
GA	Genetic algorithm
DI	Disturbance index
SI	Supporting index
DV	Disturbance vector
SV	Supporting vector
VVI	Voltage violation index

References

1. Chen, X.; Mcelroy, M.B.; Kang, C. Integrated energy systems for higher wind penetration in China: Formulation, implementation and impacts. *IEEE Trans. Power Syst.* **2017**, *33*, 1309–1319. [CrossRef]
2. Wan, Y.; Fan, C.; Dai, Y.; Li, L.; Sun, W.; Zhou, P.; Qu, X. Assessment of the joint development potential of wave and wind energy in the South China Sea. *Energies* **2018**, *11*, 398. [CrossRef]
3. Wang, L.; Vo, Q.S. Power Flow Control and Stability Improvement of Connecting an Offshore Wind Farm to a One-Machine Infinite-Bus System Using a Static Synchronous Series Compensator. *IEEE Trans. Sustain. Energy* **2013**, *4*, 358–369. [CrossRef]
4. Darabian, M.; Jalilvand, A. Improving power system stability in the presence of wind farms using STATCOM and predictive control strategy. *IET Renew. Power Gener.* **2018**, *12*, 98–111. [CrossRef]
5. Guan, L.; Li, F.; Chen, P.; Yang, J. Impacts of Offshore Wind Farms on Local Networks Voltage and Wind Power Penetration Limit. *Autom. Electr. Power Syst.* **2015**, *39*, 162–167. (In Chinese)
6. Ding, T.; Guo, Q.; Bo, R.; Sun, H.; Zhang, B.; Sciubba, E. A static voltage security region for centralized wind power integration part I: Concept and method. *Energies* **2014**, *7*, 420–443. [CrossRef]
7. Geng, H.; Liu, L.; Li, R. Synchronization and Reactive Current Support of PMSG based Wind Farm during Severe Grid Fault. *IEEE Trans. Sustain. Energy* **2018**. [CrossRef]
8. Niu, T.; Guo, Q.; Sun, H.; Wu, Q.; Zhang, B.; Ding, T. Autonomous voltage security regions to prevent cascading trip faults in wind turbine generators. *IEEE Trans. Sustain. Energy* **2017**, *7*, 1306–1316. [CrossRef]
9. Liu, P.; Li, Z.; Zhuo, Y.; Lin, X.; Ding, S.; Khalid, M.; Adio, O. Design of Wind Turbine Dynamic Trip-off Risk Alarming Mechanism for Large-scale Wind Farms. *IEEE Trans. Sustain. Energy* **2017**, *8*, 1668–1678. [CrossRef]
10. Anilkumar, R.; Devriese, G.; Srivastava, A.K. Voltage and Reactive Power Control to Maximize the Energy Savings in Power Distribution System with Wind Energy. *IEEE Trans. Ind. Appl.* **2017**, *54*, 656–664. [CrossRef]
11. Niu, T.; Guo, Q.; Sun, H.; Liu, H.; Zhang, B.; Du, Y. Dynamic reactive power reserve optimisation in wind power integration areas. *IET Gener. Trans. Distrib.* **2018**, *12*, 507–517. [CrossRef]
12. Tiwari, A.; Ajjarapu, V. Optimal Allocation of Dynamic VAR Support Using Mixed Integer Dynamic Optimization. *IEEE Trans. Power Syst.* **2011**, *26*, 305–314. [CrossRef]
13. Liu, H.; Krishnan, V.; Mccalley, J.D.; Chowdhury, A. Optimal planning of static and dynamic reactive power resources. *IET Gener. Trans. Distrib.* **2014**, *8*, 1916–1927. [CrossRef]
14. Sapkota, B.; Vittal, V. Dynamic VAR Planning in a Large Power System Using Trajectory Sensitivities. *IEEE Trans. Power Syst.* **2010**, *25*, 461–469. [CrossRef]
15. Guan, L.; Wu, L.; Li, F.; Zhao, Q. Heuristic Planning for Dynamic VAR Compensation Using Zoning Approach. *IET Gener. Trans. Distrib.* **2017**, *11*, 2852–2861. [CrossRef]
16. Wang, Y.; Li, F.; Wan, Q.; Chen, H. Reactive power planning based on fuzzy clustering, gray code, and simulated annealing. *IEEE Trans. Power Syst.* **2011**, *26*, 2246–2255. [CrossRef]
17. Huang, W.; Sun, K.; Qi, J.; Xu, Y. A new approach to optimization of dynamic reactive power sources addressing FIDVR issues. In Proceedings of the IEEE Power & Energy Society General Meeting, Washington, DC, USA, 27–31 July 2014.
18. Rather, Z.H.; Chen, Z.; Thogersen, P.; Lund, P. Dynamic reactive power compensation of large-scale wind integrated power system. *IEEE Trans. Power Syst.* **2015**, *30*, 2516–2526. [CrossRef]
19. Lind, P.G.; Vera-Tudela, L.; Wächter, M.; Kühn, M.; Peinke, J. Normal Behaviour Models for Wind Turbine Vibrations: Comparison of Neural Networks and a Stochastic Approach. *Energies* **2017**, *10*, 1944. [CrossRef]
20. Lind, P.G.; Wächter, M.; Peinke, J. Fatigue loads estimation through a simple stochastic model. *Energies* **2014**, *7*, 8279–8293. [CrossRef]
21. Croux, C.; Dehon, C. Influence functions of the Spearman and Kendall correlation measures. *Stat. Methods Appl.* **2010**, *19*, 497–515. [CrossRef]

22. Kordelas, G.; Daras, P. Robust sift-based feature matching using Kendall's rank correlation measure. In Proceedings of the 2009 16th IEEE International Conference on Image Processing (ICIP), Cairo, Egypt, 7–10 November 2009; pp. 325–328.
23. Pourbeik, P.; Sullivan, D.J.; Bostrom, A.; Sanchez-Gasca, J.; Kazachkov, Y.; Kowalski, J.; Salazar, A.; Meyer, A.; Lau, R.; Davies, D.; et al. Generic Model Structures for Simulating Static Var Systems in Power System Studies—A WECC Task Force Effort. *IEEE Trans. Power Syst.* **2012**, *27*, 1618–1627. [CrossRef]